

Analysis of mesoscale forecasts using ensemble methods

Markus Gross

*CICESE (Centro de Investigación Científica y de Educación Superior de Ensenada),
Physical Oceanography, Carretera Ensenada-Tijuana 3918, Ensenada BC 22860,
MEXICO*

Abstract

Mesoscale forecasts are now routinely performed as elements of operational forecasts and their outputs do appear convincing. However, despite their realistic appearance at times the comparison to observations is less favorable. At the grid scale these forecasts often do not compare well with observations. This is partly due to the chaotic system underlying the weather. Another key problem is that it is impossible to evaluate the risk of making decisions based on these forecasts because they do not provide a measure of confidence. Ensembles provide this information in the ensemble spread and quartiles. However, running *global* ensembles at the meso or sub mesoscale involves substantial computational resources. National centers do run such ensembles, but the subject of this publication is a method which requires significantly less computation. The *ensemble enhanced mesoscale system* presented here aims *not* at the creation of an improved mesoscale forecast model. Also it is *not* to create an improved ensemble system. Here an ensemble is created from one mesoscale forecast with the aim of interrogating the probabilities of the forecast. The diagnostics developed in this publication is the generation of the confidence intervals via cumulative probability density functions (pdf), detection of extrema and selective ensembles. The subject of this publication is the analysis of those diagnostics, their dependence on the domain size of the ensemble and the number of ensemble members. The analysis strategies introduced are termed: *subgrid ensemble enhanced mesoscale forecast*, *extreme value analysis of the ensemble pdf* and *observation constrained ensemble forecast*.

Keywords: mesoscale, forecast, precipitation, ensemble, probability density function

1. Introduction

Mesoscale forecast provide a stunning amount of detail and realism. Less dependence on parametrizations of physical processes and more resolved physics leads to a representation of weather features that appear convincing. When compared to observation, however, it is often found that locality, timing and intensity are at times not as accurate as may be desirable. As noted by Done et al. (2004), explicit treatment of convection in forecasts does not necessarily provide more accurate point forecast, but rather a more accurate depiction of the physics. Also, with sufficient lead time the single deterministic solution may vary from the observed weather to the extent that even climate means often produce smaller errors (cf Leith (1974); Epstein (2011)). This then raises the question, how reliable is this forecast? A question a single deterministic forecast cannot answer. However, sometimes it is important to know how reliable the forecast is. For example, during a week in January 2016 severe rainfall was predicted for the region of Ensenada. Some of the available deterministic models at the time predicted accumulated precipitation of 70mm or more over one or two days. This created anxiety amongst the vulnerable public. Also emergency responders were communicating these high values, demonstrating the high level of confidence attributed to these forecasts. The anxiety was increased in particular because the events occurred during the peak of a very strong el Niño event, following months of alarming speculation about the potential impacts of expected severe precipitation events commonly associated with el Niño in this region (Pavia et al., 2016). When compared with available ensemble prediction systems, Candille (2009), it could be seen that these 70mm were likely a severe over estimate of a single deterministic forecast. For risk assessment and planning, knowledge of the probabilities associated with forecast events is essential (Palmer (2002); Thielen et al. (2009)). Deterministic models cannot provide these due to their deterministic nature. Attempts are often made to compute probabilities of precipitation in the proximity by sampling the deterministic forecast. This however still assumes that the one forecast is an accurate representation of the weather at that time, which is not necessarily the case due to the chaotic nature of the weather system. An alternative to the deterministic model is an ensemble system. However, the current global ensemble systems are running at $\approx 20\text{km}$ grid resolution with an effective

resolution of 60 – 80km. Therefore, whilst producing some confidence in their forecasts and a level of certainty, the spacial uncertainty can still lead to large local forecast errors. Downscaling from the perturbed *global* model, Weidle et al. (2016), creates a significant amount of computational work, even at coarse target resolutions. This motivates the creation of a system which starts at the mesoscale, perturbs the solution (the initial condition for the ensemble) and evaluates the ensemble output. This has the advantage that it can increase the resolution and at the same time provide insight on the reliability of the forecast provided by the deterministic model. It can be reasonably expected that the high resolution nests spin up the features missing in the coarser grids in a few hours (Skamarock (2004)), providing useful forecast data for the remainder of the forecast period. Starting from the mesoscale creates an additional parameter which potentially has a detrimental impact on the output: domain size. If the domain size is small, the unperturbed boundary condition will constrain the solution and limit the statistical value of the experiment and create overly confident predictions (Kühnlein et al. (2014)). As stated above: The aim of this work is not to generate the ideal convection resolving ensemble (cf Kühnlein et al. (2014); Bouttier et al. (2012)), which inevitably needs data from global ensembles. The *ensemble enhanced mesoscale forecast* proposed here can be desirable in at least three scenarios: 1) where no sufficient resource exists to run the required *global* ensemble (or downscale each member of the *global* ensemble to the required local resolution), 2) when time is of the essence (for example in emergency response situations or forecaster-requested on-demand modeling support for the weather desk), or 3) in the case of remote embedded forecast units which rely on satellite transmission of the initial conditions.

Therefore the underlying assumption for this work is that in some situations there is not sufficient time or computing resource available to compute a high resolution convection resolving limited area model ensemble starting from global initial data. Therefore the starting point is a single deterministic mesoscale forecast. An ensemble system is then used in order to evaluate the uncertainty of this forecast without degrading the original forecasts resolution, as a neighborhood forecasting method (Theis et al. (2005)) would. Ideally the ensemble system will provide a forecast with even higher resolution as the original deterministic one, as a key aim is the forecast at a *specific location* and not area and especially not area of tens or even hundreds of kilometers squared. This high resolution, combined with the probabilistic guidance based on the intrinsic chaotic nature of the system (and not just

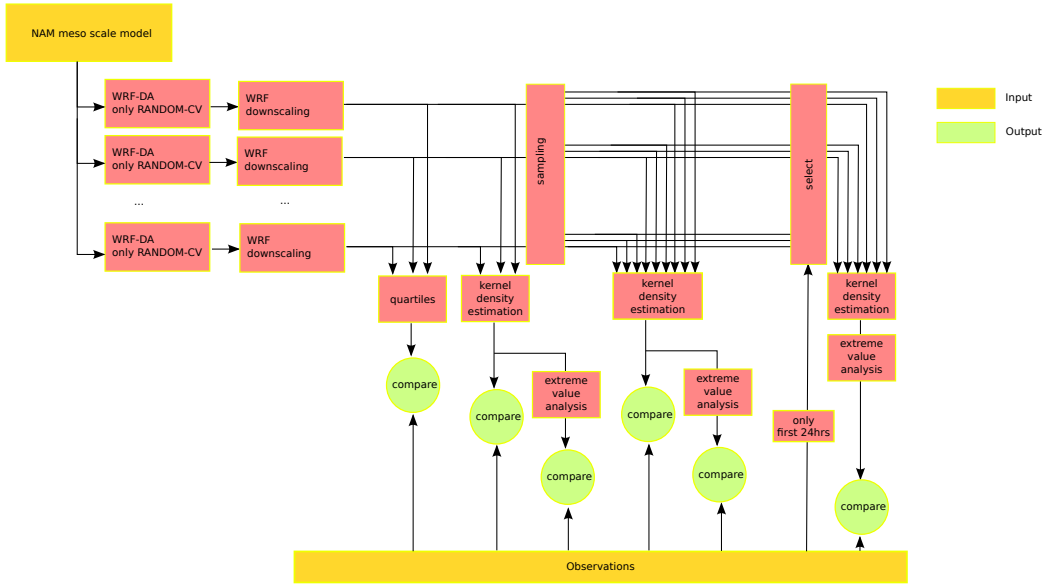


Figure 1: Methodology

some geographic evaluation) will enable the use of the forecast for emergency response. The novel aspects of this work are the introduction of what can be termed a subgrid ensemble and the further processing of this ensemble output using available observations to constrain the ensemble members and the extreme value analysis of the pdf. Here the effect of domain size, ensemble members and lead time will be illustrated, with the aim to produce *point* forecasts from a *minimal* amount of data and a *minimum* amount of computational work. Furthermore, the probabilistic guidance generated is based on the evaluation of the intrinsic chaotic nature of the weather system, which is not available in the traditional neighborhood approaches (cf. Theis et al. (2005) and Roberts and Lean (2008), for example).

In the following the methodology is presented, including the study site. This is followed by results which illustrate the methodology and demonstrate how the forecast is improved. This is followed by brief conclusions.

2. Methodology

The methodology is illustrated in Figure 1. A single deterministic forecast has been perturbed by adding random noise to the analysis in control variable space to generate initial conditions for each ensemble member.

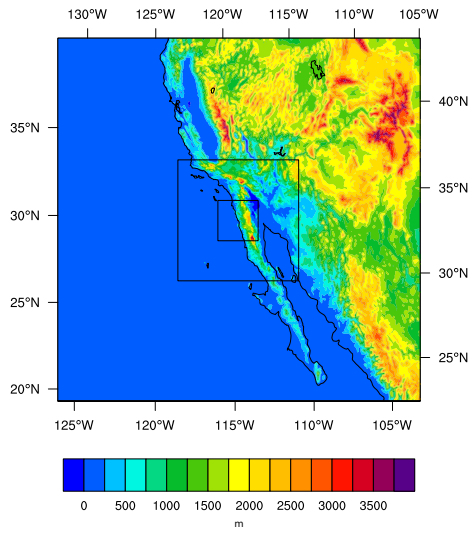
These initial conditions are then downscaled to increase the resolution and later provide grid points for sampling without surpassing the resolution of the initial data in an approach similar to neighborhood forecasting, however without degrading the resolution of forecast beyond the resolution of the initial forecast. The output is then analyzed with regard to initial domain size and number of ensemble members. Initially, the quartiles and kernel density estimation is run with an increasing number of ensemble members without any special selection procedure. A local extreme value analysis is performed and shown to indicate potential outcomes (branches) in the ensemble. Then members are selected according to the comparison against the first 24 hours of observations in order to improve the forecast for forecast hours 25 to 60.

2.1. The study area

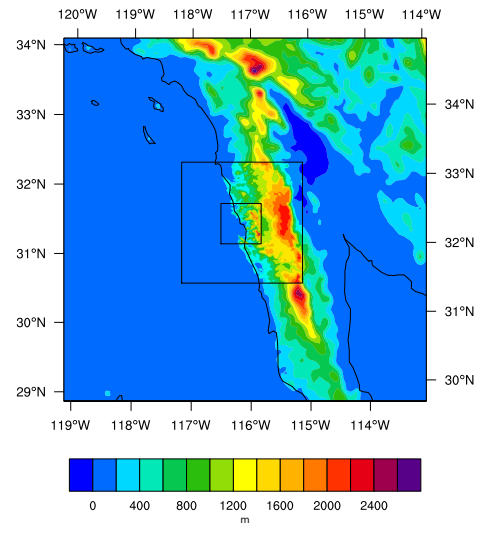
The case studies have been performed for the Port of Ensenada, Baja California, Mexico. The site was chosen due to the importance of precipitation forecasts in this area. Precipitation is usually sparse and, when it does occur, events are intense. Preparation and planning are important both for agriculture and - during extreme events - for the emergency services. The combination of the coastal setting with mountainous and desert regions in close proximity challenges the forecast models.

2.2. Model setup

The Weather Research and Forecasting (WRF) model (Skamarock et al., 2008) version 3.5.1 was run over the study area with three nests in two-way nesting. The resolutions of the domains and general model configuration is listed in Table 1. Six different domain sizes were run, $n = 40, 80, 100, 120, 140$ and 160 . This refers to a grid with $3 \times n$ grid points West to East and North to South, $9n^2$ grid points in total. The grid is centered over Ensenada, reference latitude of 31.9394 degrees and reference longitude of -116.5863 degrees. The domains, largest and smallest, are shown in Figure 2. The initial data and boundary conditions were taken from the 5km resolution North American Mesoscale (NAM) model CONUS Nest, run by the US National Weather Service - NCEP (WMC). The boundary update interval is one hour for the first 36 hours and then three hours until forecast hour 60. WRFDA (Barker et al., 2004; Huang et al., 2009), WRF Data Assimilation, was used to create the perturbed ensemble members, with only a minor modification to the random number generator seed, which was modified to create a seed of full length. No observations were assimilated into the downscaling runs.



(a) Largest domain (n=160)



(b) Smallest domain (n=40)

Figure 2: Model domains showing orography of the study area. The two nests (d02 and d03) are indicated by black lines. All domains have the same resolution for the parent (d01) and respective nests.

The initial condition is provided by a Numerical Weather Prediction model which already assimilates observations.

	d01	d02	d03
resolution	5000m	1666.66m	555m
time step	20s	20/3s	20/9s
micro physics	WSM 3-class simple ice	same as d01	same as d01
ra_lw_physics	rrtm	same as d01	same as d01
ra_sw_physics	Dudhia	same as d01	same as d01
time between radiation	1min	same as d01	same as d01
surface-layer	MM5 Monin-Obukhov	same as d01	same as d01
land-surface	thermal diffusion	same as d01	same as d01
boundary-layer	YSU	same as d01	same as d01
cumulus	Kain-Fritsch (new Eta)	same as d01	no cumulus
non-hydrostatic	.true.	.true.	.true.
dfi_opt	twice DFI (TDFI)		

Table 1: Model setup for the three domains d01, d02 and d03.

2.3. Analysis of the model output

The ensemble results were then analyzed with respect to accumulated precipitation. The ensemble mean, minimum and maximum, as well as the quartiles, probability density function (pdf) and cumulative distribution function (cdf) were compared to observations. The observations were obtained from the national meteorological service (Servicio Meteorologico Nacional), station name: P.LOPEZ ZAMORA, Ensenada, BC, Mexico, longitude: 116°36'12", latitude: 31°53'29", altitude: 32m. In all Figures presenting forecast data these observations are plotted in blue.

2.3.1. Quartiles

Quartiles are defined by the quartile function:

$$q(x_q) = p_{acc}(x = x_q) \quad (1)$$

where $q(x_q)$ is the accumulated precipitation with probability of x_q and $p_{acc}(x_i)$ is the sorted array of accumulated precipitation values from the ensemble members at discrete probabilities x_i , where the spacing and value of the x_i depends on the ensemble size. $p_{acc}(x = x_q)$ is then evaluated using linear interpolation.

2.3.2. Pdf and cdf

The distribution of precipitation is truncated at zero as it cannot be negative. Therefore a truncated kernel density estimation (kde) is performed, with lower bound zero. A normal Gaussian kernel is assumed, such that the pdf ϕ is

$$\phi = \frac{1}{\sqrt{2\pi}} \exp^{-\frac{x^2}{2}} . \quad (2)$$

Linear combination correction (Jones (1993)) has been performed to represent the truncated distribution, ϕ_t , which has a lower bound of zero. The obtained pdf has the advantage that it can be readily integrated into the cdf $\hat{\phi}$

$$\hat{\phi}(x) = \int_0^x \phi_t(u) du \quad (3)$$

and more accurate quartiles can be obtained by evaluation of this integral.

2.3.3. Subgrid ensemble enhanced mesoscale forecast

In the sub-grid ensemble the ensemble size is extended. Not by adding more ensemble members, but by allowing for a geographic uncertainty. The ensemble members from neighboring grid points are combined to form a larger ensemble.

Since the ensemble downscales the mesoscale forecast the solution can be sampled without reducing the resolution beyond the original mesoscale forecast. This sampling is similar to the neighborhood forecasting approach of Theis et al. (2005). However, here the resolution is at least the resolution of the driving mesoscale model, not less. Furthermore it is important to note that here the chaotic nature of the weather system is sampled by the ensemble, which is not the case in the traditional neighborhood forecasting approach, nor in any other method which attempts to extract probabilities from deterministic data. The third domain can be sampled in $(3 \times 3)^2 = 81$ points before the resolution of the original mesoscale forecast is reached. This is the *subgrid ensemble enhanced mesoscale forecast*.

2.3.4. Extreme value analysis of the ensemble pdf

The pdf obtained from the ensemble can be further analyzed for local extrema (maxima). These extrema will be shown to carry useful information, highlighting potential outcomes which would be lost if only the quartiles and ensemble mean would be considered.

2.3.5. Constrained ensemble

Finally the data is analyzed taking observations into account. Ensemble members are selected according to their difference to observation. A ranking, s_e , is computed for each ensemble member e over the first 24 samples (here one per hour)

$$s_e = \sum_{i=1}^{24} s_{e,i},$$

where

$$s_{e,i} = \begin{cases} 1 & \text{if } \text{obs}(t_i) - \sigma < p_{acc}(e, t_i) < \text{obs}(t_i) + \sigma \\ 0 & \text{otherwise} \end{cases} \quad (4)$$

with obs , t , i , σ , $p_{acc}(e, t_i)$ denoting the observed accumulated precipitation, discrete time and its index i , standard deviation of all ensemble members at the respective time step and accumulated precipitation of ensemble member e at time t_i , respectively. If $s_e > s_{thresh}$, where s_{thresh} is a threshold to be defined, the member is retained in the ensemble. The threshold is a free parameter, as illustrated in the results below. The aim of this final exercise is to improve the forecast at a time when observations are available. Naturally, the error or uncertainty is largest with longer lead time and some improvement becomes necessary. It will be shown that this can be achieved using this selection process.

3. Results and Discussion

First, a comparison of model versus observations under varying domain and ensemble sizes for two key dates, initial time 4th of January 00:00 UTC and initial time of 7th of January 00:00 UTC are presented.

Then the benefit of the *subgrid ensemble enhanced mesoscale forecast* is shown. This improves the ensemble, meaning that more outcomes resemble the observations. Line plots of the time series of the ensemble members suggest some clustering, i.e. some outcomes appear more likely than others.

Following this observation the local maxima in the pdf are analyzed, the *extreme value analysis of the ensemble pdf*. This reveals several possible outcomes and their bifurcation points.

Finally, in order to improve the later part of the forecast, observations made during the first 24 hours are “assimilated” into the geographically extended ensemble and results of this exercise are also presented.

3.1. Point forecasts

Precipitation is amongst the most difficult variables to predict and yet arguably one of the most important aspects of numerical weather forecasting. This difficulty is often glossed over by reporting the probability of precipitation (PoP; National Weather Service (1984)), which is computed by evaluating the precipitation over a larger geographic area and time window (and is associated with great difficulty in its communicating to and understanding by the general public (Joslyn et al. (2009))). However, this has only limited success and, more critically, significantly less value for the individual who is mostly interested in precipitation in very specific areas and less concerned about precipitation elsewhere. For this reason, the interest here lies with forecasts at specific locations, which can then also be readily compared to ground-based observations (it is less clear how PoP can be compared to observations other than satellite observations with their larger margin of error). Here the focus is on accumulated precipitation, which simplifies the comparison as it relaxes the timing component, the “Double Penalty Issue” (Mass and Kuo, 1998):

- The precipitation event may *not appear* at exactly the same time as in the observation and then
- *it appears* in the model (minutes earlier or later) when it does not appear in the observational record.

This complicates objective verification of instantaneous precipitation significantly.

In Figures 3 and 4 the time series of accumulated precipitation are plotted. Each of the plots shows six components: Minimum and maximum across all ensemble members, ensemble mean (red), 25th and 75th quartile for the cpd (c.f. Equation 3) shown in red shading, 25th and 75th quartile for the interpolation approach (c.f. Equation 1) shown in green shading and the observations (blue). The sub panels present the information for the different domain sizes, $n=40$ to 160, top to bottom, and number of ensemble members considered, five to 19, left to right.

3.1.1. Initial time 04 January 2016 00:00 UTC

For initial time 04 January 2016 00:00 UTC the forecasts appear to not capture the high amount of rainfall and it is difficult to derive a clear domain size and ensemble member count sensitivity. Interestingly, the medium

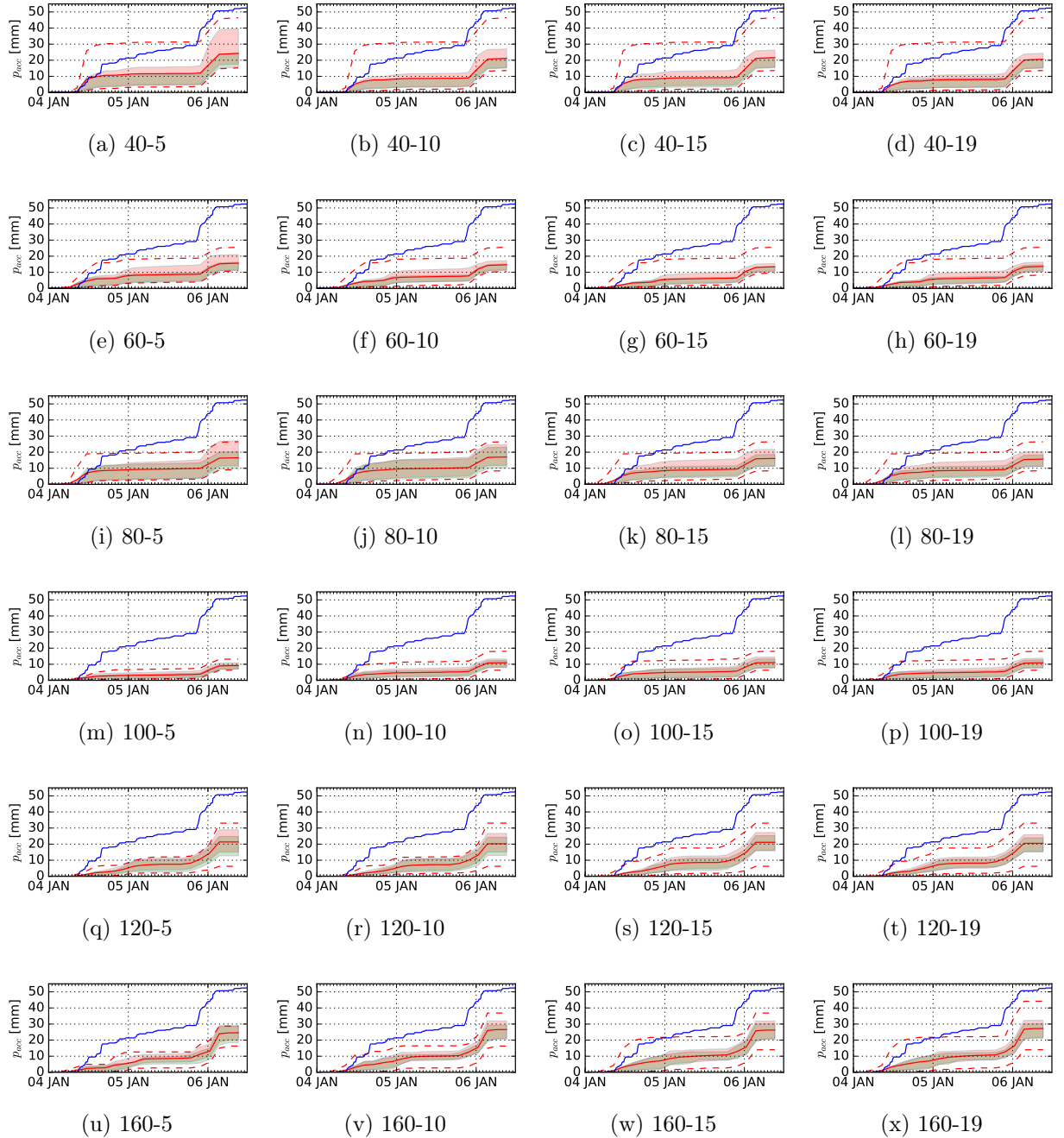


Figure 3: Accumulated precipitation, p_{acc} , for initial time: 04 Jan 2016 00:00 UTC, domain d03. Dashed lines: Minimum and maximum across all ensemble members, cumulative density function interval from 0.25 until 0.75 in red shading and quartiles in green shading. Observations are plotted in blue and ensemble mean in red. The caption of the sub panels indicated domain size followed by ensemble size (members considered).

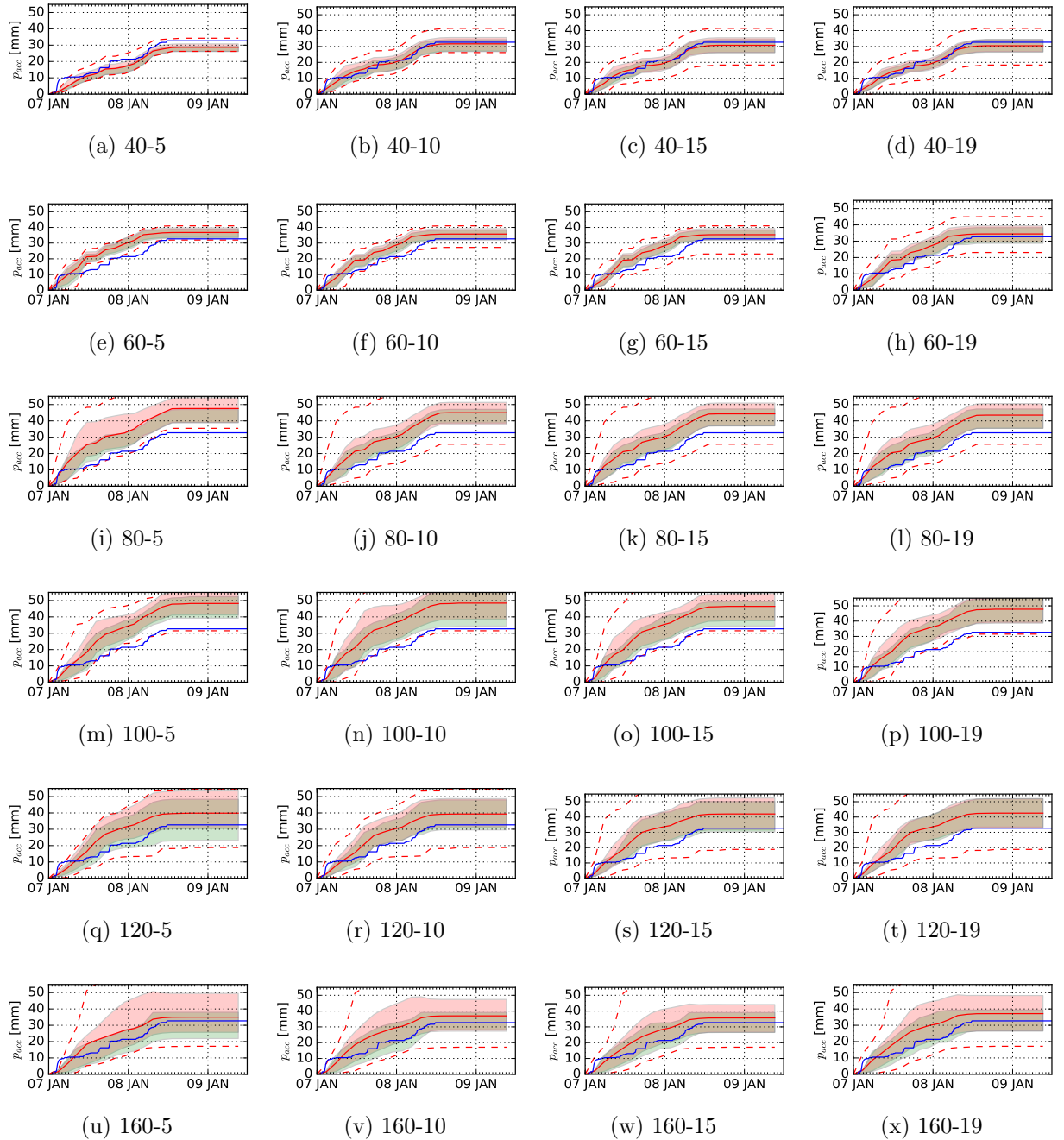


Figure 4: Accumulated precipitation, p_{acc} , for initial time: 07 Jan 2016 00:00 UTC, domain d03. Dashed lines: Minimum and maximum across all ensemble members, cumulative density function interval from 0.25 until 0.75 in red shading and quartiles in green shading. Observations are plotted in blue and ensemble mean in red. The caption of the sub panels indicated domain size followed by ensemble size (members considered).

domain sizes are outperformed by both, the smaller and larger domains. It may appear here as if all the ensemble members for 04 January were missing the real weather, certainly in the ensemble mean. It will be shown later that this is an effect of the meaning. Here the ensemble certainly was improved by adding more members and increasing the domain size. It is not clear if increasing the domain much more (ignoring for a while that the NAM domain does not extend much more into the region) and adding significantly more members will eventually improve on the second half of the forecast. Whilst there is improvement when comparing the panels in Figure 3, the improvement is small.

3.1.2. Initial time 07 January 2016 00:00 UTC

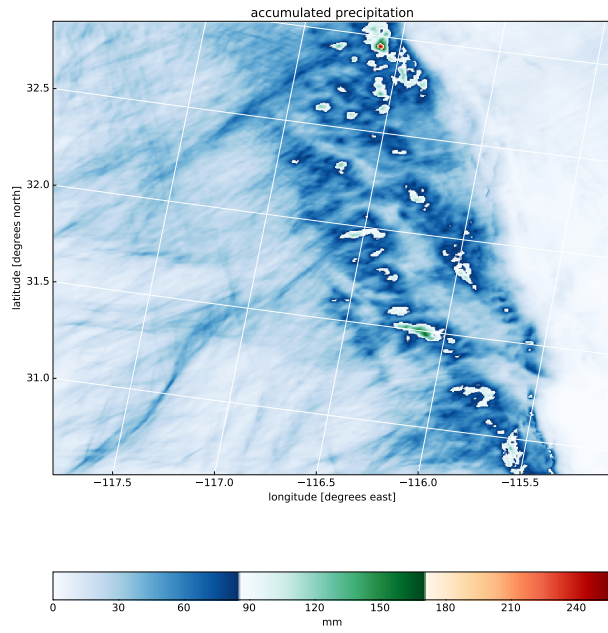
The results are different for the 07 January 2016 00:00 UTC data set. There it can be readily observed how the ensemble is overly constrained for the small domain sizes by its lateral boundary conditions (cf. Kühnlein et al. (2014)), which are unperturbed. For the small domain sizes the ensemble spread, the difference between minimum and maximum, is small. Coincidentally, for the initial time of 07 January 2016 00:00 UTC the results are close to the observations, however, this in itself does not make them more likely. With the low spread of the small domain ensemble it simply means that the mesoscale forecast was already close to observations. The spread increases as the domain size passes $n = 80$. With the ensemble mean staying close to the observations this then increases the confidence.

3.2. Spatial uncertainty

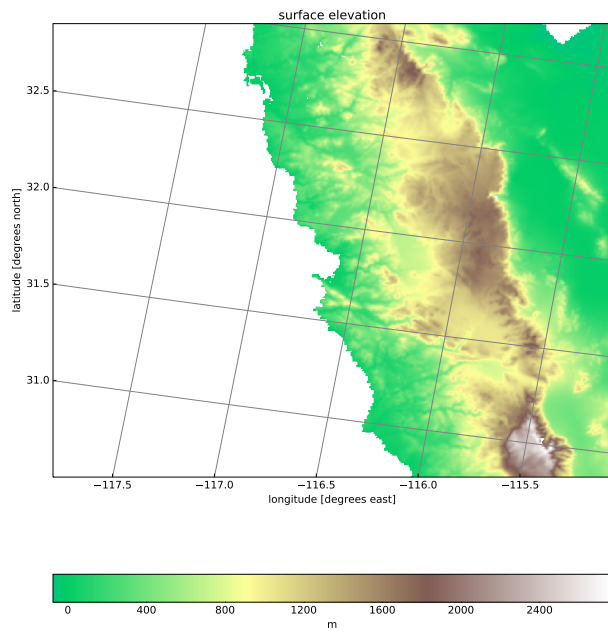
The two examples above showed that the ensemble alone is not always sufficient. To improve the forecast there are two options: Increase the ensemble members or utilize the spatial variation. Here increasing the ensemble members does not appear as promising, in particular since the aim is to reduce the computational effort.

Since the computational effort of the downscaling increases linearly but the spatial sampling available increases quadratically the *subgrid ensemble enhanced mesoscale forecast* is more cost effective.

Figure 5 shows that the spatial distribution of the precipitation is indeed highly non-uniform. A spatial sampling error therefore can have a large impact on the forecast accuracy. Figure 6 shows the effect of 3×3 subgrid sampling. The sampling generates a 9 grid point ensemble with $20 \times 9 = 180$ members and compares it to the non-sample, single point 20 member

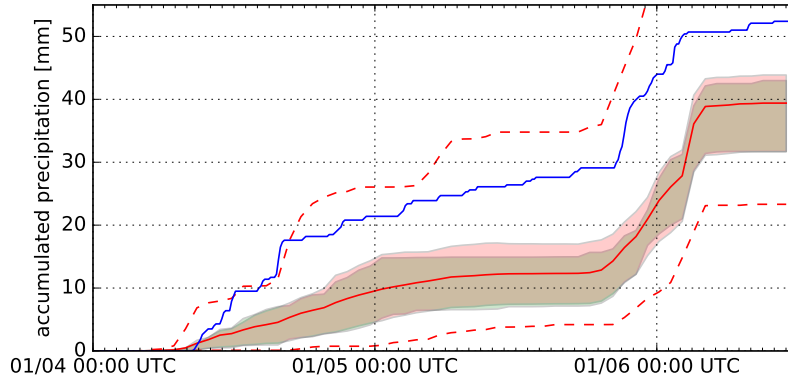


(a) Accumulated precipitation at the end of the 62hr forecast for the largest domain ($n = 160$) with highest resolution (d03).

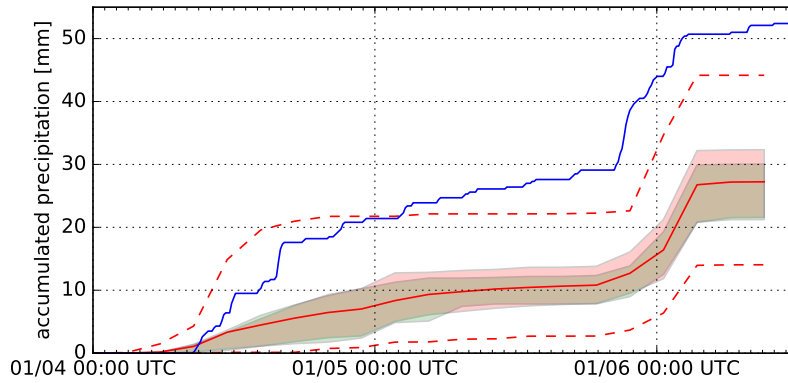


(b) Terrain in the highest resolution domain

Figure 5: Spatial distribution of precipitation



(a) Subgrid enhanced



(b) Point ensemble

Figure 6: Precipitation quartiles for the large domain ensemble. initial time: 04 Jan 2016 00:00 UTC. The observed precipitation is plotted in blue, the cumulative density function interval from 0.25 until 0.75 in transparent red fill, 0.25 to 0.75 quartiles in transparent green fill, ensemble minimum and maximum with a dashed red line and the ensemble mean with a solid red line.

ensemble for the forecast run with initial date 04 January 2016, the most difficult case due to its extreme precipitation. It can be seen that the subgrid sampling has clearly improved the forecast. The 25% and 75% quartiles have moved up, in the direction of the observations and the minimum and maximum now nearly always incorporate the observations. Overall, however, the precipitation for this extreme case is still underpredicted by a factor of about two.

3.3. Modal analysis: Extract potential branches

Clustering can be observed in the line plots of the time series for the 3×3 grid point array in Figure 7. The time series for accumulated precipitation has been color coded according to the location of the grid point. For example at the 4th of January, 16:00UTC, clusters can be identified. It would not be surprising if these clusters would all belong to the same grid points. However, the color coding shows clearly this is not the case. This means that each cluster has contributions from several ensemble members of the other grid boxes. Analyzing the pdf for local extrema extracts these clusters. This allows the separation into scenarios, i.e. several possible predictions of high (or similar/significant) likelihood.

It can be seen clearly that some of these branches trace the observations closer than others.

In Figure 8 the pdf for each time step was analyzed for local extrema. Each data point represents a time step and extrema. That is, if there are two points per time step there were two local maxima, if there are three then three local maxima were observed. Several alternative outcomes can be observed in this *extreme value analysis of the ensemble pdf*. It can be seen how one of the potential outcomes comes very close to the observed time series. For the first 24hours the observations are within less than one standard deviation (σ) of the forecast, for forecast hours (fh) 24 to 48 within less than $\sigma/2$, focusing on the upper branches. Initially the upper branch would not appear a sensible choice, due to its significantly lower probability. However, as this is accumulated precipitation it would be equally unrealistic to accept the good match in the first 24 hrs and then choose the lower branch for the remaining period, which would require a reduction of accumulated precipitation at approximately fh 18, which is physically not possible.

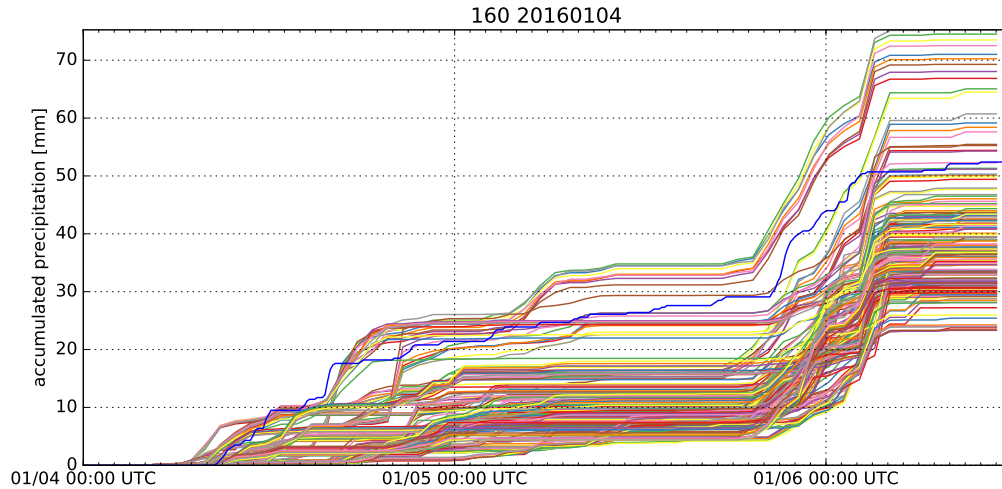


Figure 7: Geographic and perturbation ensemble. Initial time: 04 Jan 2016 00:00 UTC. The blue line represents the observations in grid point i, j and each color of the remaining lines represents a unique geographical location (ii, jj) , with $i - 1 \leq ii \leq i + 1$ and $j - 1 \leq jj \leq j + 1$.

3.4. Assimilation of observations

In the analysis above one of the possible scenarios comes close to the observations, at least until 00:00 UTC 06 January 2016. However, it was not the scenario with the highest probability, and, furthermore, the spread in between the scenarios increased significantly with lead time. Performing the ensemble runs and their analysis takes time. The question to be answered here is if the forecast for days 2 and 2.5 can be improved if the ensemble members are selected by their correlation with the observations in day one (c.f. Equation 4). This is termed *observation constrained ensemble forecast* from here onward.

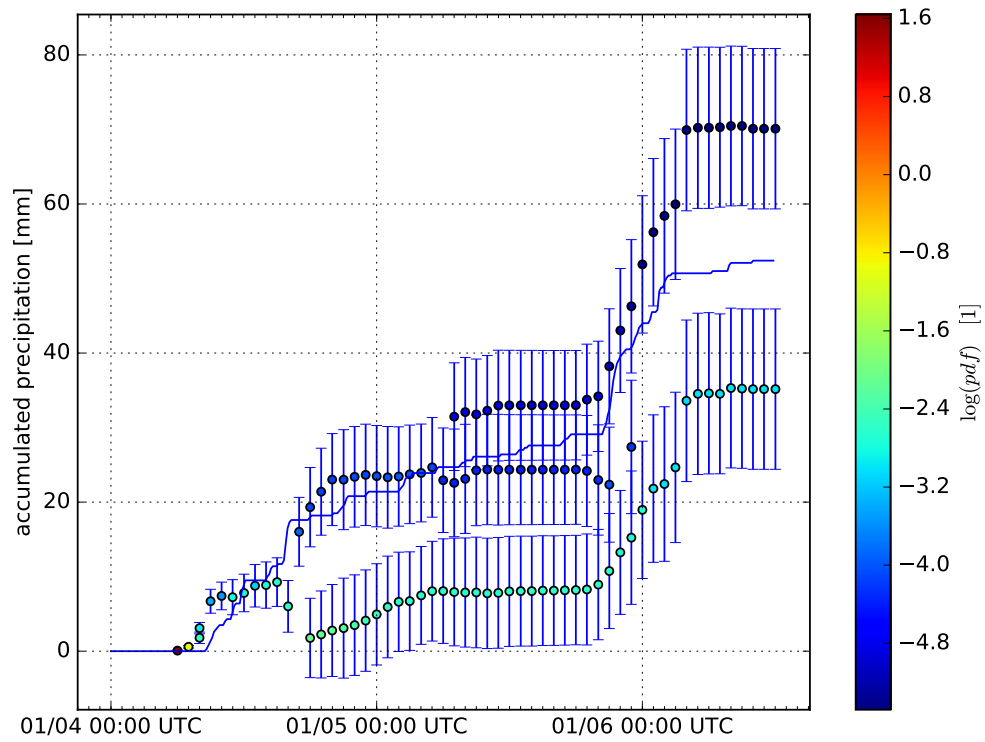


Figure 8: Analysis of extrema of the pdf. The error bars represent one standard deviation of the ensemble members, the observed precipitation is plotted in blue. The color coding represents the logarithm of the value of the pdf at the location of the maxima.

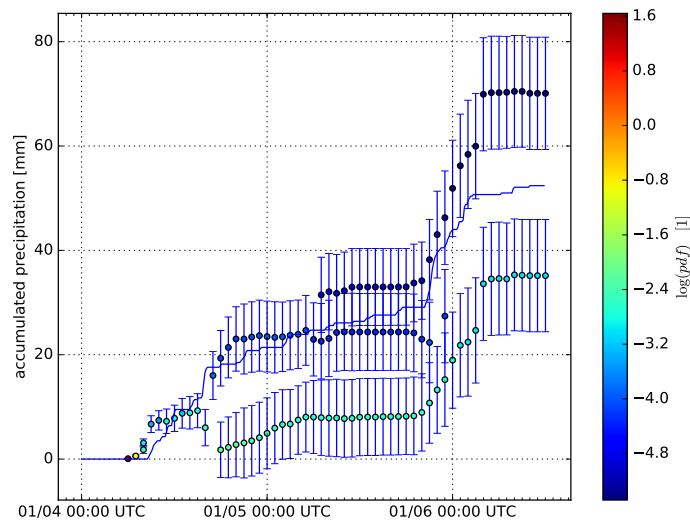
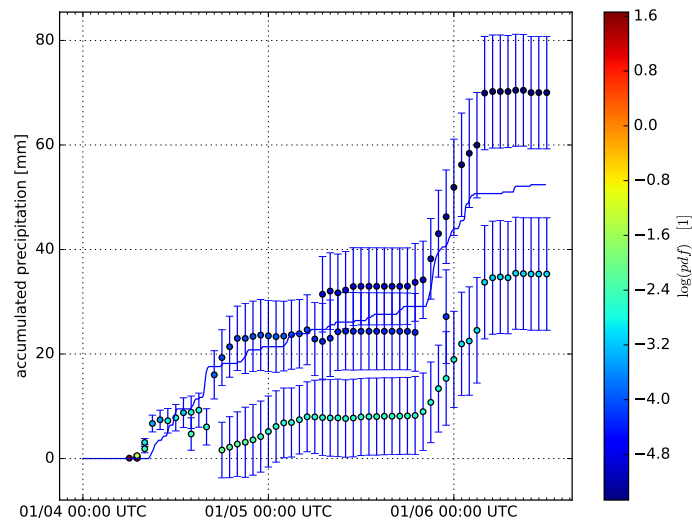
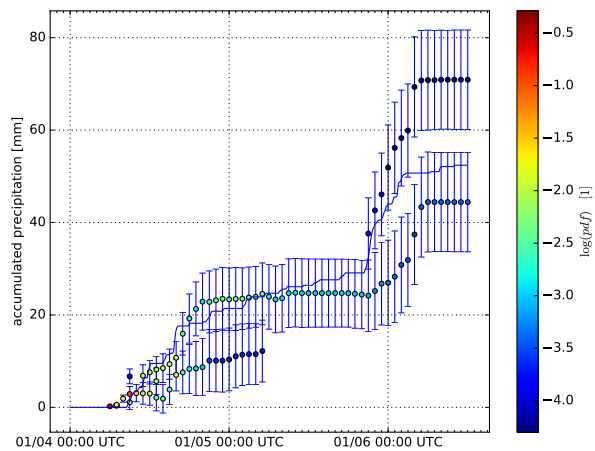
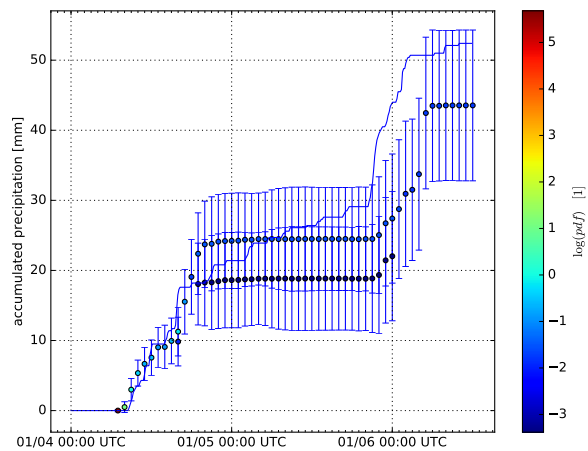
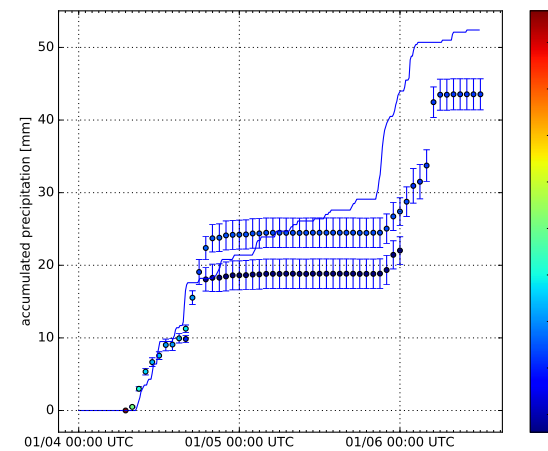
(a) $S_{thresh} = 5$ (b) $S_{thresh} = 10$ (c) $S_{thresh} = 15$ (d) $S_{thresh} = 20$ (e) $S_{thresh} = 20$

Figure 9: Selecting ensemble members according to the first 24 hrs. The error bars in subpanel (a-d) represent one standard deviation of the original full member ensemble. In subpanel e the error bars denote the standard deviation of the selected ensemble members only.

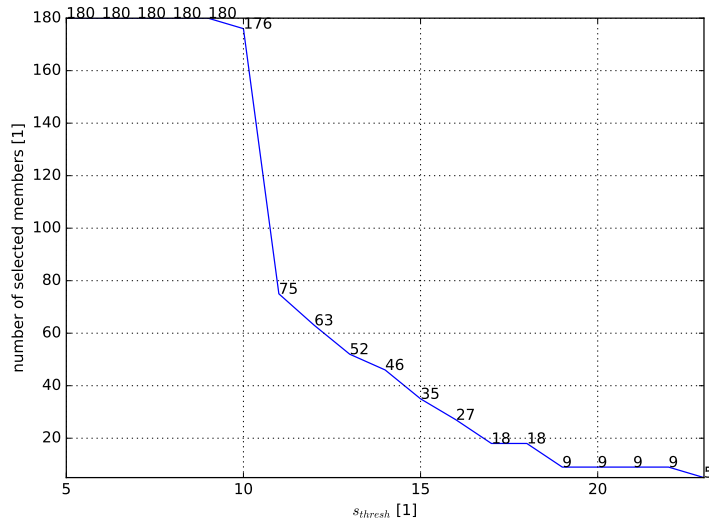


Figure 10: Number of ensemble members selected for the modal analysis above versus the minimum number of time steps within the first 24hours that agree to within ± 1 standard deviation with the observations, s_{thresh} , as in Equation 4.

Figure 9 shows how the constraining of the ensemble yields an improved forecast. With the requirement that at least 20 time steps of the first 24 be within two standard deviations the severely overestimating branch has been removed and the observations are within less than one standard deviation of the maxima. Figure 9e reproduces the plot for a match of more than 20 time steps and plots the standard deviation of the selected ensemble members as error bars. The number of ensemble members remaining after selection is shown in Figure 10.

4. Conclusions

It was shown how a single deterministic forecast can be augmented with probabilities and analyzed with respect to likely outcomes. At small domains the effect of the lateral boundary condition dominates, as expected. With larger domains the ensemble spread widens. For some cases the *ensemble enhanced mesoscale forecast* already provides good guidance, as shown with the example of the 7 January 2016 case. The 04 January 2016 case was more challenging. Extending the ensemble, acknowledging a spatial uncertainty,

slightly improved the guidance in the *subgrid ensemble enhanced mesoscale forecast*. However, it still failed to emphasize that the high (50mm, in contrast to the extreme 80mm) precipitation event may be more justified. Analyzing the local maxima in the cpd effectively highlighted these alternate scenarios and differentiated them from the remaining ensemble members. It would have been impossible to deduce this from the line plots of the whole extended ensemble (Figure 7). Finally it was shown how an *observation constrained ensemble forecast* significantly improved the longer lead time of the forecast (fh24 to fh60), taking the observations available in the first 24hours into account.

It is hoped that these ideas will provide a product which will aid the forecaster when deciding, from the mix of different models and sources of information available, on balanced conclusion that lead to more accurate forecasts.

Acknowledgments

The author would like to acknowledge the National Super Computer Center (CNS) of IPCYT A.C. for providing access to the super computer facility Thubat Kaal, and Dr Julio Scheinbaum of CICESE for kindly providing access to the chaman cluster. The author would like to thank Dr Magar and Dr Turrent Thompson for the constructive discussions and proofreading of the manuscript.

References

- D.M. Barker, W. Huang Y. R. Guo, and Q. N. Xiao. A three-dimensional (3DVAR) data assimilation system for use with MM5: Implementation and initial results. *Mon. Wea. Rev.*, (132):897–914, 2004.
- François Bouttier, Benoît Vié, Olivier Nuissier, and Laure Raynaud. Impact of stochastic physics in a convection-permitting ensemble. *Monthly Weather Review*, 140(11):3706–3721, 2012. doi: 10.1175/MWR-D-12-00031.1. URL <http://dx.doi.org/10.1175/MWR-D-12-00031.1>.
- Guillem Candille. The multiensemble approach: The naefs example. *Monthly Weather Review*, 137(5):1655–1665, 2009. doi: 10.1175/2008MWR2682.1. URL <http://dx.doi.org/10.1175/2008MWR2682.1>.

- James Done, Christopher A. Davis, and Morris Weisman. The next generation of NWP: explicit forecasts of convection using the weather research and forecasting (WRF) model. *Atmospheric Science Letters*, 5(6):110–117, 2004. ISSN 1530-261X. doi: 10.1002/asl.72. URL <http://dx.doi.org/10.1002/asl.72>.
- Edward Epstein. Stochastic dynamic prediction. *Tellus A*, 21(6), 2011. ISSN 1600-0870. URL <http://www.tellusa.net/index.php/tellusa/article/view/10143>.
- X.Y. Huang, Q. Xiao, D.M. Barker, X. Zhang, J. Michalakes, W. Huang, T. Henderson, J. Bray, Y. Chen, Z. Ma, J. Dudhia, Y. Guo, X. Zhang, D.J. Won, H.C. Lin, and Y.H. Kuo. Four-dimensional variational data assimilation for WRF: Formulation and preliminary results. *Mon. Wea. Rev.*, 137:299–314, 2009.
- M. C. Jones. Simple boundary correction for kernel density estimation. *Statistics and Computing*, 3(3):135–146, 1993. ISSN 1573-1375. doi: 10.1007/BF00147776. URL <http://dx.doi.org/10.1007/BF00147776>.
- Susan Joslyn, Limor Nadav-Greenberg, and Rebecca M. Nichols. Probability of precipitation: Assessment and enhancement of end-user understanding. *Bulletin of the American Meteorological Society*, 90(2):185–193, 2009. doi: 10.1175/2008BAMS2509.1. URL <http://dx.doi.org/10.1175/2008BAMS2509.1>.
- C. Kühnlein, C. Keil, G. C. Craig, and C. Gebhardt. The impact of down-scaled initial condition perturbations on convective-scale ensemble forecasts of precipitation. *Quarterly Journal of the Royal Meteorological Society*, 140(682):1552–1562, 2014. ISSN 1477-870X. doi: 10.1002/qj.2238. URL <http://dx.doi.org/10.1002/qj.2238>.
- C. E. Leith. Theoretical skill of monte carlo forecasts. *Monthly Weather Review*, 102(6):409–418, 1974. doi: 10.1175/1520-0493(1974)102<0409:TSOMCF>2.0.CO;2. URL [http://dx.doi.org/10.1175/1520-0493\(1974\)102<0409:TSOMCF>2.0.CO;2](http://dx.doi.org/10.1175/1520-0493(1974)102<0409:TSOMCF>2.0.CO;2).
- Clifford F. Mass and Ying-Hwa Kuo. Regional real-time numerical weather prediction: Current status and future potential. *Bulletin of the American Meteorological Society*, 79(2):253–263, 1998. doi: 10.1175/1520-0477(1998)

- 079<0253:RRTNWP>2.0.CO;2. URL [http://dx.doi.org/10.1175/1520-0477\(1998\)079<0253:RRTNWP>2.0.CO;2](http://dx.doi.org/10.1175/1520-0477(1998)079<0253:RRTNWP>2.0.CO;2).
- National Weather Service. *Zone and local forecasts. NWS Operations Manual W/OM15.*, 1984. URL www.nws.noaa.gov/wsom/manual/archives/NC118411.HTML. part C, chapter 11.
- T. N. Palmer. The economic value of ensemble forecasts as a tool for risk assessment: From days to decades. *Quarterly Journal of the Royal Meteorological Society*, 128(581):747–774, 2002. ISSN 1477-870X. doi: 10.1256/0035900021643593. URL <http://dx.doi.org/10.1256/0035900021643593>.
- Edgar G. Pavia, Federico Graef, and Ramón Fuentes-Franco. Recent ensemble precipitation relationships in the mediterranean california border region. *Atmospheric Science Letters*, 17(4):280–285, 2016. ISSN 1530-261X. doi: 10.1002/asl.656. URL <http://dx.doi.org/10.1002/asl.656>.
- Nigel M. Roberts and Humphrey W. Lean. Scale-selective verification of rainfall accumulations from high-resolution forecasts of convective events. *Monthly Weather Review*, 136(1):78–97, 2008. doi: 10.1175/2007MWR2123.1. URL <http://dx.doi.org/10.1175/2007MWR2123.1>.
- William C. Skamarock. Evaluating mesoscale nwp models using kinetic energy spectra. *Monthly Weather Review*, 132(12):3019–3032, 2004. doi: 10.1175/MWR2830.1. URL <http://dx.doi.org/10.1175/MWR2830.1>.
- William C. Skamarock, Joseph B. Klemp, Jimy Dudhia, David O. Gill, Dale M. Barker, Michael G. Duda, Xiang-Yu Huang, Wei Wang, and Jordan G. Powers. A description of the advanced research WRF version 3. Technical Report NCAR/TN-475+STR, NCAR, June 2008.
- S. E. Theis, A. Hense, and U. Damrath. Probabilistic precipitation forecasts from a deterministic model: a pragmatic approach. *Meteorological Applications*, 12(3):257–268, 2005. ISSN 1469-8080. doi: 10.1017/S1350482705001763. URL <http://dx.doi.org/10.1017/S1350482705001763>.
- J. Thielen, K. Bogner, F. Pappenberger, M. Kalas, M. del Medico, and A. de Roo. Monthly-, medium-, and short-range flood warning: testing

the limits of predictability. *Meteorological Applications*, 16(1):77–90, 2009. ISSN 1469-8080. doi: 10.1002/met.140. URL <http://dx.doi.org/10.1002/met.140>.

Florian Weidle, Yong Wang, and Geert Smet. On the impact of the choice of global ensemble in forcing a regional ensemble system. *Weather and Forecasting*, 31(2):515–530, 2016. doi: 10.1175/WAF-D-15-0102.1. URL <http://dx.doi.org/10.1175/WAF-D-15-0102.1>.